Available online at www.sciencedirect.com
SCIENCE DIRECT®
Materials Science and Engineering C 23 (2003) 757–762
MATERIALS SCIENCE & ENGINEERING C
www.elsevier.com/locate/msec

Clustering and formation of nano-precipitates in dilute aluminium and magnesium alloys

T.J. Bastow[a,b,*], S. Celotto[c]

[a] CSIRO Manufacturing Science and Technology, Locked Bag 33, South Clayton MDC, Victoria 3169, Australia
[b] School of Physics and Materials Engineering, Monash University, Clayton, Victoria 3168, Australia
[c] Department of Engineering, Materials Science and Engineering, University of Liverpool, Brownlow Hill, Liverpool L69 3BX, UK

Abstract

A nuclear magnetic resonance (NMR) method is described for monitoring the evolution of nano-scale precipitate structures in dilute aluminium and magnesium-based alloys. Three examples are given of recent work in this field: (i) ^{63}Cu detection of Guinier–Preston zones (GPZs) and θ-phases in Al(Cu), (ii) ^{27}Al detection of γ-phase ($Mg_{17}Al_{12}$) formation in Mg(Al) alloys and (iii) ^{45}Sc detection of Al_3Sc formation in Al(Sc) alloys.

Keywords: Light alloys; Precipitation; Intermetallics; Nuclear magnetic resonance

1. Introduction

Light metals such as aluminium and magnesium, of prime importance to the aerospace, marine and automotive industries, are intrinsically soft and easily deformed plastically. To make such metals strong, durable, corrosion resistant, etc., they are alloyed with amounts ~ 1–5 at.% of another element, which are only sparingly soluble in the host matrix, generally forming solute–host or solute–solute compounds, initially at least on the nanometer scale, as precipitates after low-temperature heat treatment.

From a post hoc examination of the aluminium alloy crankcase of the Wright brothers aircraft in the 1920s onwards, the fundamental importance of very fine precipitation in light metals as a strengthening (toughening) agent for these metals has been fully realized. It was quickly realized that the role of the precipitates is to block dislocation movement, which is the principal mechanical failure mechanism. It is then evident that nano-scale precipitates will be the most effective (cover more bases) at blocking the movement of dislocations, and that as the precipitates grow (coarsen) on extended heat treatment, having exhausted the solute content of the host, their effectiveness decreases since the dislocations can then move in the spaces between the more sparsely occurring large precipitate grains.

The metallurgist's conventional tools for examination of the extent and nature of the precipitates have been hardness measurements, optical microscopy of polished sections and transmission electron microscopy of thin foils. Because of the tenuous, low-dimensional and poorly ordered nature of some of many of these precipitates, especially in their early stages of formation, X-ray diffraction is not widely used as an analytical tool in this context. Electron diffraction/microscopy gives the dimensions and crystallographic orientation of the precipitate crystallites relative to the host lattice but views only a very small (~ 1 μm^3) region of the material at a time. A bulk measurement of the concentration of the various precipitate species is generally not easily extracted from diffraction measurements.

The experiments outlined below illustrate, with three examples, an analytical technique, based on nuclear magnetic resonance (NMR), which yields the concentration and type of the precipitates that form in aluminium and magnesium alloys of industrial use. These alloys belong to the large class of alloys for which the desired mechanical properties can be achieved by heat treatment or age hardening. In the examples below, the precipitates are detected by the NMR signal from the nucleus of one of the solute species; specifically ^{63}Cu in the Al(1.7 at.% Cu) [1], ^{27}Al in

* Corresponding author. CSIRO Manufacturing Science and Technology, Locked Bag 33, South Clayton MDC, Victoria 3169, Australia. Tel.: +61-3-9545-2680; fax: +61-3-9544-1128.
E-mail address: tim.bastow@csiro.au (T.J. Bastow).

0928-4931/$ - see front matter © 2003 Elsevier B.V. All rights reserved.
doi:10.1016/j.msec.2003.09.140

the Mg-based alloy AZ91 or Mg(9 at.% Al, 0.4 at.% Zn) [2] and ^{45}Sc in Al(0.06 at.% Sc) [3]. The NMR spectrum in all cases consists of a line from the solute atom in solid solution and one or more lines from the various (crystallographically distinct) precipitate structures. The fundamental reason that these lines can be spectroscopically easily resolved is that the line shift (for metals, the Knight shift) mechanism is the contact interaction [4], which enhances the nuclear resonance shifts, over their values in non-metals, by a factor of order 50.

For the Al(Cu) alloys, monitoring the evolution of the ^{63}Cu line for the Cu in the first ordered structure to form from the Cu in solid solution, i.e., the Guinier–Preston zones (GPZ), yields information about the preliminary clustering process. For the Mg(Al) alloys, on the other hand, the first (and only) precipitate that forms from Al in solid solution, i.e., γ-phase $Mg_{17}Al_{12}$, shows no ^{27}Al NMR spectroscopic evidence of an intervening clustering stage. The ^{45}Sc NMR spectra of very dilute Al(Sc) alloys indicate no GPZ formation but suggest that in the early stages of heat treatment, the Al_3Sc precipitate morphology may be dendritic.

All spectra were taken at room temperature. The specimens were rapidly cooled to room temperature at the end of each aging period and then loaded into the spectrometer.

The assignment of the NMR lines to their respective phases in the various alloys is discussed in detail in Refs. [1–3].

2. Experimental

The alloy NMR specimens were prepared from bulk alloy specimens by filing and sieving to 160 μm. The powder (~ 500 mg per specimen) was then sealed in a glass tube under argon and solution treated at 535 °C for [Al(Cu)], 420 °C [Mg(Al)] and 640 °C [Al(Sc)] before quenching rapidly (the glass shattering on entry) into iced water. The water was then filtered off and the powder washed with ethanol and dried at room temperature. The alloy powders were then heat treated for times and at temperatures indicated in the figures.

The spectrometer was a Bruker 400 operating around 106.02 MHz (^{63}Cu) and 104.24 MHz (^{27}Al) in a nominal field of 9.4 T. All measurements were performed with a static sample using either a two-pulse echo sequence [Al(Cu)], Al(Sc) or single pulse Bloch decays [Mg(Al)]. The spectra were then obtained by Fourier transform to give the absorption lineshape. The pulse widths were typically 2–3 μs with an irradiation bandwidth of 500–330 kHz. The loading caused by Joule losses in the metal particles of the specimen lowered the *Q*-factor of the probe, decreasing the sensitivity but increasing the probe bandwidth to approximately 2 MHz. The reference zero shift for ^{63}Cu was for diamagnetic solid CuCl, $AlCl_3{\bullet}(6H_2O)^{3+}$ for ^{27}Al and $ScCl_3$ (aq) for ^{45}Sc. The Knight shifts for the spectra in the figures below are indicated in parts per million (ppm).

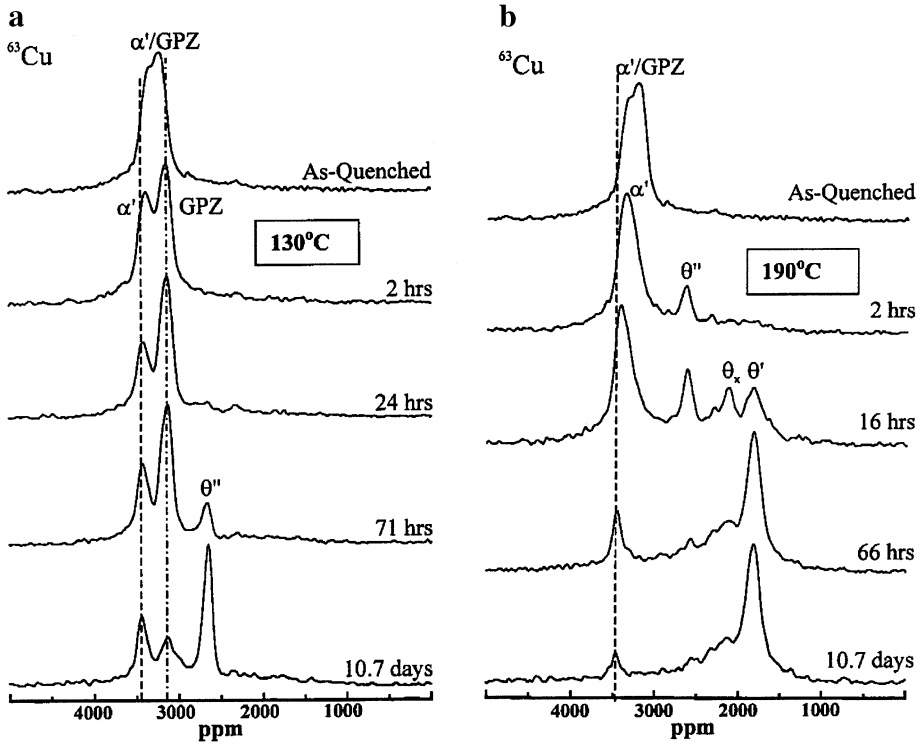

Fig. 1. ^{63}Cu NMR spectra for solution treated and quenched Al(1.7 at.% Cu): (a) aged at 130 °C, and (b) aged at 190 °C.

3. Discussion

3.1. Al(1.7 at.% Cu)

3.1.1. 130 °C Aging

The progression in phase development from the as-quenched state up to 10.7 days aging is shown in Fig. 1(a). A spectrum taken immediately after quenching revealed a barely resolved doublet of which the high-frequency (left side) component is due to Cu in substitutional sites in the α-phase of Al, and the low-frequency (right side) component is due to Cu in the GPZ that form readily at room temperature. After 2 h of aging, the α-phase and GPZ components of the doublet had moved apart, and this separation has increased after 24 h aging and does not increase subsequently. This behaviour implies that during the first few hours at 130 °C, the Cu atoms are coming out of solid solution and clustering, prior to the formation of the GPZ, viz. disks (one atom thick, 5–10 nm diameter) on (100) planes of the Al α-phase. A schematic illustration of GPZ and subsequent θ-phases is shown in Fig. 2.

After 71 h at 130 °C another peak, assigned to the θ″-phase appears. On further aging, the θ″-phase then grows mainly at the expense of the GPZ phase. Note that the display in Fig. 1 (and in the spectra displayed in Figs. 3 and 4) sets the largest peak at constant height, so that the distribution of solute between the various phases is given by the ratio of areas under the respective peaks. After 10.7 days at 130 °C, the phase distribution has essentially reached its equilibrium and no subsequent development is observed. It can be seen that although the GPZ peak rapidly

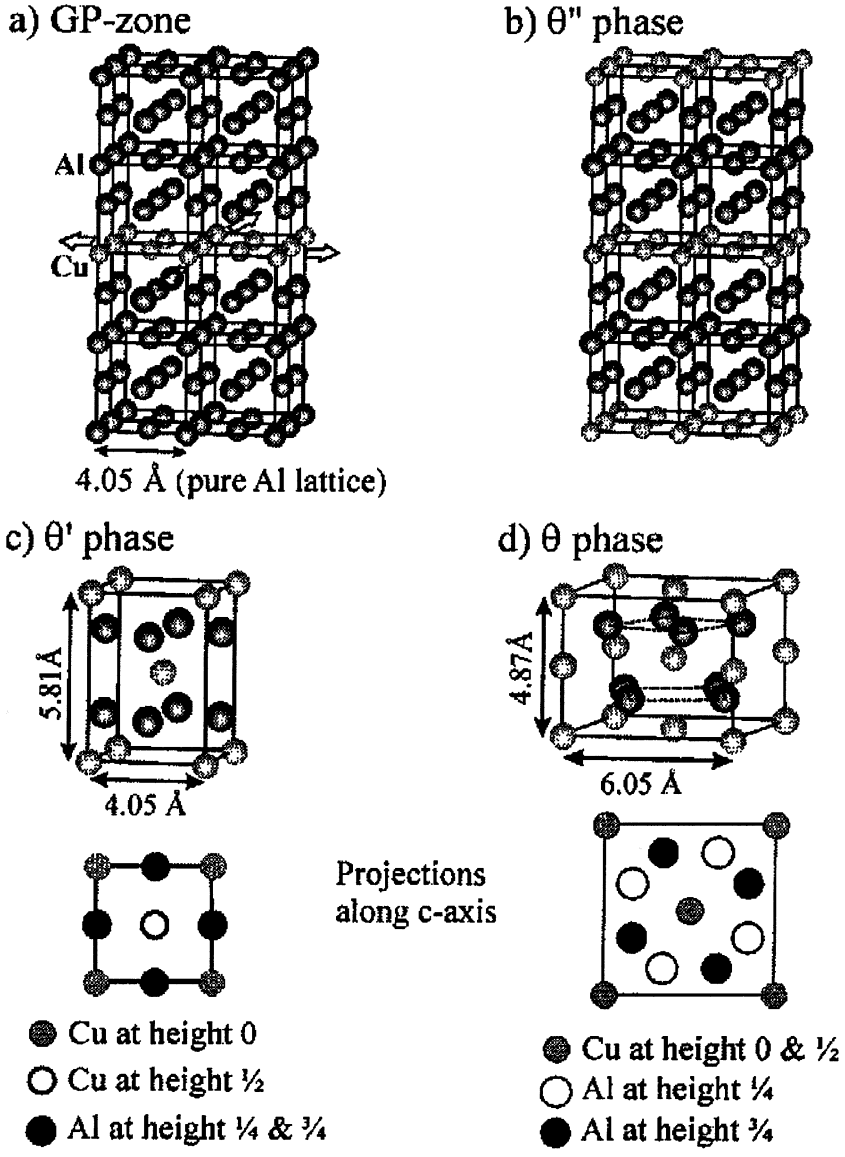

Fig. 2. Schematic structures of (a) GPZ, (b) θ″-phase, (c) θ′phase and (d) θ-phase.

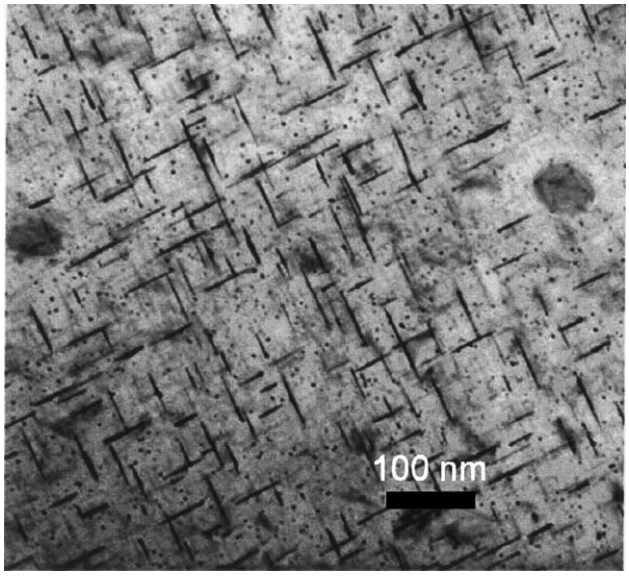

Fig. 3. Transmission electron micrograph of Al(1.7 at.% Cu) aged at 150 °C for 100 h showing a mixture of θ″- and θ′-phase (orthogonal linear features parallel to [100] and [010].

reaches its final shift value, the α-phase peak gradually asymptotes to a final value as the Cu is gradually exhausted from the Al host lattice, the electronic state of the remaining Cu becomes increasingly well defined as an impurity state and the valence electron/atom ratio for the system approaches 3 from below.

3.1.2. 190 °C Aging

At 190 °C, the phase evolution rate from the as-quenched state is considerably increased.

Two hours of aging has dissolved the GPZ leaving Cu mainly in α-phase and a minor amount in θ″-phase. After 16 h, two extra peaks appear; one due to θ′-phase, of which thin platelets are beginning to appear, and the other assigned to Cu at the surface of these platelets and labeled θ_x. As the aging progresses, the θ″-phase line disappears, the θ′-phase line increases and the θ_x line subsides into the background, consistent with the coarsening of the θ′ precipitates and the diminution of the fractional contribution of surface Cu. Beyond 66 h of aging, no development occurs apart from a diminution apart from a further diminution of the Cu in α-phase.

A transmission electron micrograph of the alloy annealed at 150 °C for 100 h is displayed in Fig. 5. The precipitates at this stage consist of a mixture of θ″- and θ′-phases shown as linear features of order 100 nm in length parallel to [100] and [010], which are the cross sections of the largely two dimensional morphology of these phases.

The ultimately stable θ-phase (Al_2Cu), which is completely incoherent with the Al host lattice, requires aging at higher temperatures (~ 370 °C). The ^{63}Cu spectrum is readily observed [1], but from the materials viewpoint, this phase is of minor interest since by that stage the alloy is heavily over-aged and the mechanical properties are well below optimal.

3.2. Mg(9 at.% Al, 0.4 at.% Zn)

The maximum solid solubility of aluminium in magnesium is 11.9 at.% Al at the eutectic temperature of 437 °C, and the equilibrium concentration at 200 °C is 2.6 at.% Al, so that a relatively large amount of Al is available for precipitation. When the Al content exceeds the solubility limit in Mg the γ-phase intermetallic $Mg_{17}Al_{12}$ forms as a precipitate. Although $Mg_{17}Al_{12}$ can be NMR detected by its characteristic three line ^{25}Mg spectrum [5], its presence is most easily monitored via the single line ^{27}Al spectrum [5].

For Mg(9 at.% Al, 0.4 at.% Zn) in the as-quenched state the spectrum consists of a single line (Fig. 4a) corresponding to Al in random solid solution in hexagonal close packed Mg. Additional experiments [2] on a series of binary Mg(Al) alloys from 10 to 0.25 at.% Al show the ^{27}Al Knight shift increasing uniformly as the Al content decreased, corresponding to a uniform shift in average valence electron/atom ratio towards 2 from above, providing an independent calibration of [Al] in terms of Knight shift.

The ^{27}Al line became much narrower below 1 at.% Al as the dispersive effects of varying Al clustering decreased and the most frequently occurring Al site was one in which an

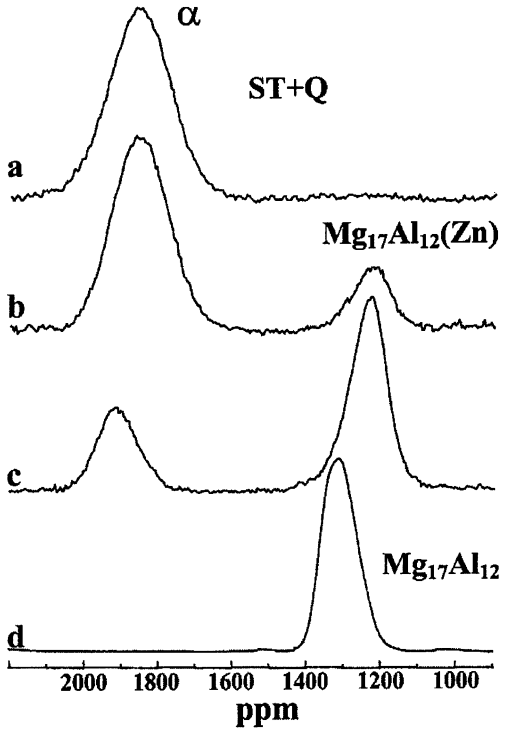

Fig. 4. ^{27}Al NMR spectra for Mg(9 at.% Al, 0.4 at.% Zn): (a) solution treated and quenched; aged at 200 °C for (b) 4 h and (c) 250 h; (d) stoichiometric $Mg_{17}Al_{12}$.

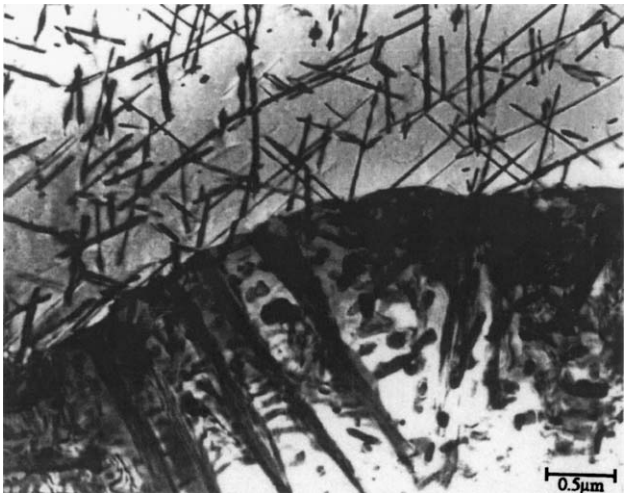

Fig. 5. Transmission electron micrograph of AZ91 aged at 200 °C for 4 h showing a region of discontinuous (below) and continuous (above) precipitation.

Al atom was surrounded by at least two nearest neighbour shells of Mg.

Aging at 200 °C produces a additional line (Fig. 4b) corresponding to the presence of γ-phase $Mg_{17}Al_{12}$ precipitates. These occur in two morphologies corresponding to discontinuous (Fig. 5, below) and continuous (Fig. 5, above) precipitation. Continuous precipitation is the dominant process at longer aging times and consists of long lath-shaped plates of order 100–1000 nm in length. The ^{27}Al spectrum records both discontinuous and continuous precipitation at the same shift value due to the short range of the interactions causing the shift.

The Knight shift for γ-phase $Mg_{17}Al_{12}$ prepared by arc melting is slightly different to that for the γ-phase formed in the alloy due to the presence of zinc in the alloy (Fig. 4d). The divalent Zn (which is added to accelerate precipitation and give greater peak hardness) displaces the trivalent Al in the γ-phase and alters the electron to atom ratio, which contributes to determining the shift. If Mg was displaced, this would not affect *e*/*a*. Varying the Zn content yields a smooth decrease in the ^{27}Al Knight shift from its value for zero Zn [2]. Note that there are no peaks in the ^{27}Al spectrum at early aging times, which could be attributed to an intermediate phase occurring before the equilibrium γ-phase, such as a GP zone.

After 250 h, (Fig. 4C) the precipitate peak is about twice the integrated intensity of the α-phase line, which has moved to higher shift corresponding to the dilution of Al in the α-phase due to the formation of more γ-phase. Further aging at 200 °C does not noticeably increase the γ-phase fraction.

3.3. Al(0.06 at.% Sc)

The solid solubility of Sc in Al is very low, being 0.23 at.% Sc at the eutectic temperature and decreasing rapidly with decreasing temperature. The sensitivity of ^{45}Sc NMR allows an accurate measurement of scandium solubility at the Al-rich end of the phase diagram [3]. The precipitate that forms on slow cooling from the melt in an ingot of Al(Sc) is the intermetallic phase Al_3Sc [6]. The line is relatively narrow, consistent with the cubic coordination of Sc by Al in this structure.

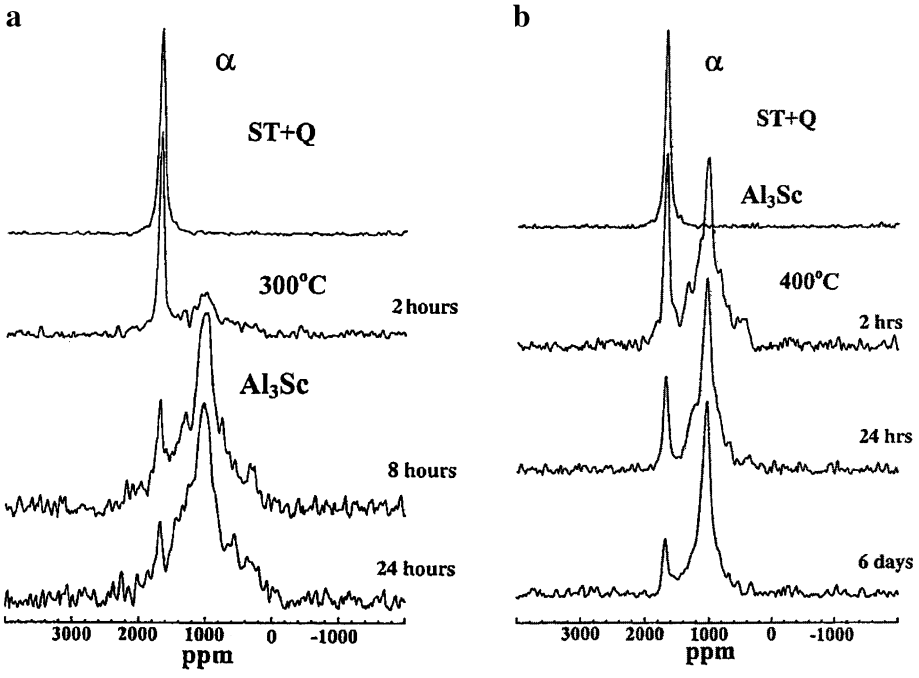

Fig. 6. ^{45}Sc NMR spectra for solution treated and quenched Al(0.06 at.% Sc) aged at (a) 300 °C and (b) 400 °C.

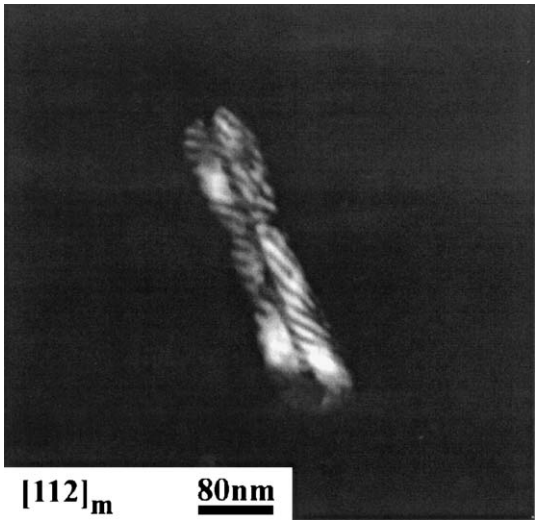

Fig. 7. Transmission electron micrograph of Al_3Sc particle in Al(0.06 at.% Sc) aged at 400 °C for 24 h.

In this section, we concentrate on the alloy Al(0.06 at.% Sc). The ^{45}Sc spectrum for the as-quenched state of this alloy exhibits a single line corresponding to Sc in random solid solution in the Al α-phase host lattice (Fig. 6). This state appears quite metastable at room temperature in that no NMR-visible precipitation appears to form at ambient laboratory conditions for extended periods. After aging at 300 °C (Fig. 6a) for 2 h, an additional weak ^{45}Sc broad line centred at the Al_3Sc shift [6]. Further aging at this temperature substantially increases the intensity of this line at the expense of the line for Sc in α-phase Al. The width of the line suggests a dendritic morphology for the Al_3Sc in which the extended nature of the wings is caused by the distribution of immediate atomic environments (a mixture of vacancies and Al atoms) around the Sc atom.

The 300 °C aging spectra should be compared with those observed after 400 °C aging for corresponding times (Fig. 6b), where the Al_3Sc line is sharper and more compact, corresponding to better crystallinity of the precipitates. A transmission electron micrograph of an alloy specimen annealed at 400 °C for 24 h is shown in Fig. 7 [7]. After 6 days at 400 °C, the Al_3Sc lineshape was essentially identical to that obtained from an Al_3Sc specimen prepared by arc melting the elemental constituents [4]. Note that at no stage was a separate line observed, which could be attributed to GP zones.

4. Conclusions

NMR provides an element-specific, structure-sensitive probe of phases that form in dilute aluminium- and magnesium-based alloys. These phases can be detected spectroscopically at extremely early stages in their formation when their physical dimensions are sufficiently small to make them difficult to resolve by electron microscopy and identify by electron diffraction. The clustering that precedes GPZ formation can be observed in Al(Cu) alloys and the presence of the metastable two-dimensional GPZ and θ″-phases are clearly established. The absence of any precursor phases to the equilibrium precipitate phase is confirmed for Mg(Al) and Al(Sc), although the presence of dendritic morphology in the early stages of Al_3Sc formation can be inferred from the lineshape. A remarkable feature of the spectra is that the resonance lines due to the various precipitate phases are resolved due to a shift amplification based on the electron–nucleus contact interaction. This resolution allows a quantitative measurement of the phase content of the specimen by simple integration under the peaks in the spectra, and also a measurement of the amount of solute remaining in substitutional sites in the host lattice.

Acknowledgements

We are grateful to Roger Lumley for providing the TEM micrographs of the precipitation in Al(1.7 at.% Cu) alloy.

References

[1] T.J. Bastow, S. Celotto, Acta Mater. 51 (2003) 4621.
[2] T.J. Bastow, S. Celotto, Acta Mater. 49 (2001) 41.
[3] S. Celotto, T.J. Bastow, Phil. Mag. A80 (2000) 1111.
[4] C.P. Slichter, Principle of Magnetic Resonance, 3rd ed., Springer-Verlag, New York, 1990.
[5] T.J. Bastow, M.E. Smith, J. Phys., Condens. Matter 7 (1995) 4929.
[6] T.J. Bastow, C.T. Forwood, M.A. Gibson, M.E. Smith, Phys. Rev. B58 (1998) 6.
[7] S. Celotto, Acta Mater. 48 (2000) 1775.